

# Systematic Variation of Hybrid APCs into YBCO Thin Films for Improving the Vortex Pinning Properties

Alok K. Jha, Kaname Matsumoto, Tomoya Horide, Shrikant Saini, Paolo Mele, Yutaka Yoshida, and Satoshi Awaji

**Abstract**—The effect of hybrid (columnar and spherical) artificial pinning centers (APCs) on the vortex pinning properties of YBCO thin films is studied in the present manuscript on the basis of variation of critical current density ( $J_c$ ) with applied magnetic field and also with the orientation of the applied magnetic field. YBCO+BSO3% composite target is used for preparing film with 1-D (columnar) APCs while the same composite target is modified by putting two differently sized (2.2 area% and 3 area%)  $Y_2O_3$  sectored pieces for preparing films having different concentrations of 3-D (spherical) APCs along with 1-D APCs. Film consisting of only 1-D APCs exhibits enhanced in-field  $J_c$  values as compared to the one without any APC and the ones consisting of hybrid APCs exhibit even better  $J_c$ -B characteristics with increase in the fraction of 3-D APCs.  $F_{pmax}$  values increase systematically with incorporation of 1-D and 1-D + 3-D APCs and it also shifts towards higher applied magnetic fields. Film with 1-D APCs exhibits strong  $J_c$  peak at  $\Theta = 0^\circ$  (H//c-axis) whereas films consisting of hybrid APCs exhibit enhanced  $J_c$  at all the investigated angular regime. A possible mechanism of vortex pinning in samples with hybrid APCs is also discussed suggesting the role of 1-D and 3-D APCs.

**Keywords**—Hybrid APCs, thin films, YBCO, vortex pinning

## I. INTRODUCTION

IN ORDER to use  $YBa_2Cu_3O_{7-\delta}$  (YBCO) superconducting thin films for widespread technological applications, the critical current density ( $J_c$ ) needs to be significantly improved at elevated temperatures over wide range of applied magnetic fields [1]. Many methods have been successfully employed to improve the flux pinning properties of YBCO thin films and majority of these methods essentially aim to incorporate nanoscale secondary phase inclusions into YBCO superconducting film matrix which generate artificial pinning centers (APCs). The nanoinclusions of several materials such

as  $Y_2O_3$  [2],  $YBa_2CuO_5$  [3],  $BaZrO_3$  [4], [5],  $BaSnO_3$  [6], [7],  $YBaNbO_6$  [8], [9], etc. have been demonstrated to enhance the vortex pinning properties of YBCO films deposited by pulsed laser deposition (PLD) technique. Self-assembled nanocolumns of secondary phase materials such as  $BaZrO_3$  (BZO),  $BaSnO_3$  (BSO),  $YBaTaO_6$  (YBTO) etc. have resulted in the improvement of  $J_c$  values when the applied magnetic field is along the  $c$ -axis. However, the  $J_c$  performance also needs to be improved when the magnetic field is oriented along the intermediate angular regime (between  $ab$  plane and  $c$ -axis). In a recent report, Horide *et al* [10] have shown that the incorporation of hybrid structures (1-D nanocolumns together with 3-D nanoparticles) into YBCO thin film on metallic tapes reduces the  $J_c$  anisotropy.

In this paper, we present the microstructural and transport properties of YBCO thin films incorporating both 1-D APC material:  $BaSnO_3$  (BSO) and 3-D APC material:  $Y_2O_3$  (YO). To introduce 1-D and 3-D APCs into the YBCO films, mixed target as well as surface modified targets has been used in the present study. The effect of systematic incorporation of hybrid APCs on the critical current properties of YBCO films on single crystal substrates is discussed in the present manuscript.

## II. EXPERIMENTAL DETAILS

Thin films of YBCO and its nanocomposites with BSO and BSO+ $Y_2O_3$  have been deposited on single crystal  $SrTiO_3$  (STO) substrates using PLD technique (KrF excimer laser,  $\lambda = 248$  nm). The deposition conditions have been described elsewhere [9]. For the deposition of pure YBCO thin film, a pristine YBCO target was ablated for 9,000 laser pulses. For YBCO+BSO nanocomposite films, YBCO+BSO(3%) mixed target was used and for YBCO+BSO+ $Y_2O_3$  films, the surface of the same YBCO+BSO target is modified with two different sizes of sectored YO pieces: 2.2 area % and 3 area % which are referred as YOA and YOB in the paper onwards. As the target is rotated, the  $Y_2O_3$  portion is periodically ablated allowing the formation of YO nanoparticles together with BSO nanocolumns in the YBCO film matrix. The microstructure and cross-sections of YBCO+BSO and YBCO+BSO+YO nanocomposite films have been studied using transmission electron microscopy (TEM). Transport properties of these thin film samples have been measured using four-probe method by a Physical Property Measurement System (PPMS, Quantum Design). A voltage criterion of  $1 \mu V cm^{-1}$  has been used to obtain the critical current values. Angular dependence of  $J_c$  of all the thin film samples was

Manuscript revised November 05, 2014. This work was supported by KAKENHI, Grant-in-Aid for Science Research (S), Grant Number 23226014.

A.K. Jha, K. Matsumoto and T. Horide are with Department of Materials Science and Engineering, Kyushu Institute of Technology, Tobata-ku, Kitakyushu 804-8550 JAPAN (e-mail: akjha@post.matsc.kyutech.ac.jp; matsuo@post.matsc.kyutech.ac.jp; horide@post.matsc.kyutech.ac.jp) Phone: +81-80-3984-7120

S. Saini and P. Mele are with Institute for Sustainable Science and Development, Hiroshima University, Higashi-Hiroshima 739-8530 JAPAN (email: ssaini@hiroshima-u.ac.jp; pmele@hiroshima-u.ac.jp)

Y. Yoshida is with Department of Energy Engineering and Science, Nagoya University, Nagoya 464-8063 JAPAN (email: yoshida@nuee.nagoya-u.ac.jp)

S. Awaji is with Institute for Materials Research, Tohoku University, Sendai 980-8577 JAPAN (email: awaji@imr.tohoku.ac.jp)

measured at 77 K, 1 T and 65 K, 3 T using the same voltage criterion.

### III. RESULTS AND DISCUSSION

In order to compare the microstructure of the single APC and hybrid APC samples, the typical cross-sectional TEM images of YBCO+BSO and YBCO+BSO+YOB films have been presented in Fig. 1(a) and (b) respectively. In both the TEM images, the formation of nanocolumnar structures can be observed clearly. However, in fig. 1(b), spherical nanostructures are also visible which are supposed to be  $Y_2O_3$  nanoparticles. The formation of some planar defects is also observed which are usually generated and have been reported earlier also [9]. Using both mixed target and surface modified target approach, both columnar and spherical APCs are incorporated into the YBCO film matrix.

The variation of  $J_c$  with applied magnetic field for YBCO, YBCO+BSO and YBCO+BSO+YO films at 77 K and 65 K are presented in fig. 2. At 77 K, the self-field  $J_c$  values of all the studied samples vary between 1.6-2.8 MA.cm<sup>-2</sup>. It can be seen that the  $J_c$  values for YBCO+BSO nanocomposite films are enhanced significantly as compared to that for pure YBCO film and this enhancement is more prominent at higher applied magnetic field. For YBCO+BSO+YO films, this enhancement is even higher although these have less self-field  $J_c$  values. With increasing YO content in the samples, the  $J_c$ -B characteristic improves further. It can be concluded that the BSO nanorods and YO nanoparticles both are effective to improve the critical current properties of YBCO films.

In fig. 3, the variation of pinning force density ( $F_p$ ) as a function of applied magnetic field for YBCO, YBCO+BSO and YBCO+BSO+YO films at (a) 77 K and (b) 65 K are presented. At 77 K,  $F_{pmax}$  for YBCO film is 2.86 GN.m<sup>-3</sup> whereas it increases to 8.25, 8.64 and 10.91 GN.m<sup>-3</sup> for YBCO+BSO, YBCO+BSO+YOA and YBCO+BSO+YOB films respectively. Similarly, at 65 K,  $F_{pmax}$  for YBCO film is 13.6 GN.m<sup>-3</sup> whereas it increases to 43.38, 52.80, and 60.13 GN.m<sup>-3</sup> for YBCO+BSO, YBCO+BSO+YOA and YBCO+BSO+YOB films respectively. There is significant increase in the  $F_p$  values of the films consisting of 1-D and 1-D + 3-D (hybrid) APCs indicating the effectiveness of both BSO nanocolumns and YO nanoparticles as strong pinning centers. Apart from the significant increase in the  $F_{pmax}$  values, the applied magnetic field at which  $F_{pmax}$  occurs is shifted towards higher values for YBCO films consisting of hybrid APCs, which means that pinning is more effective at higher applied magnetic field in films consisting of hybrid APCs.

In fig. 4, the reduced  $F_p$  ( $=F_p/F_{pmax}$ ) is plotted as a function of applied magnetic field for both the temperatures: 77 K (a), and 65 K (b). The variation of reduced  $F_p$  eliminates the effect of absolute  $F_p$  value. The shifting of  $F_{pmax}$  values towards higher magnetic fields is marked by dotted arrows in the figures. Shifting of  $F_{pmax}$  values towards higher applied magnetic field can be understood in terms of the vortex densities in the samples. Usually, vortices are occupied by the nanorods

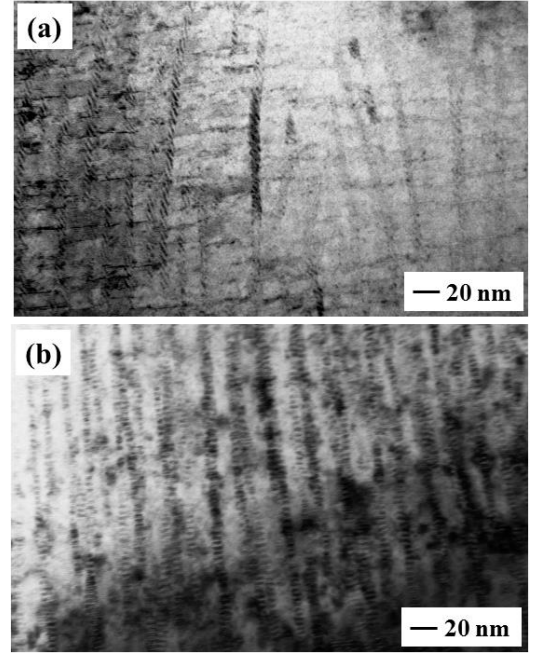


**FIG. 1** Cross-sectional TEM images of (a) YBCO+BSO3% and (b) YBCO+BSO3%+YOB films. The formation of nanocolumns in both the cases and that of nanoparticles in sample with hybrid APCs can be observed.

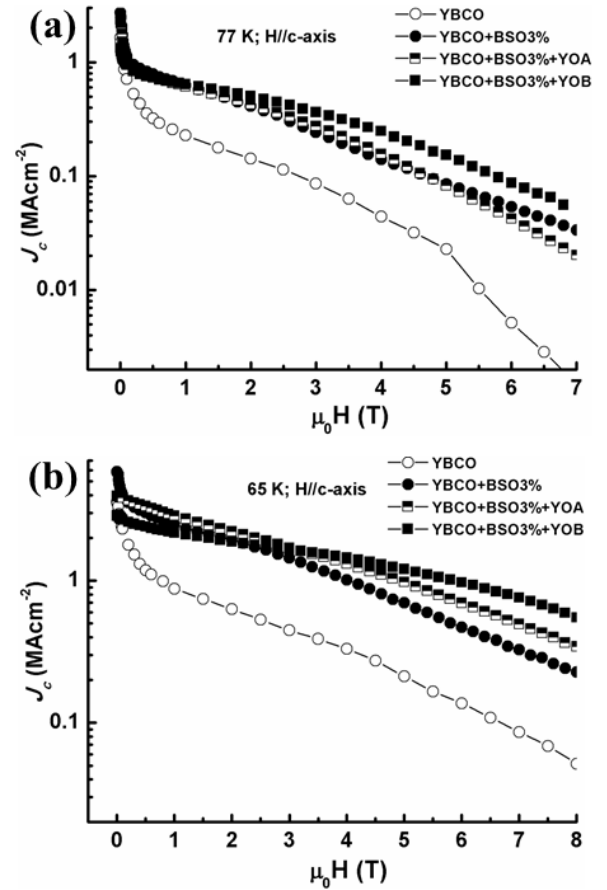


**FIG. 2** Variation of  $J_c$  with applied magnetic field for YBCO, YBCO+BSO3%, YBCO+BSO3%+YOA and YBCO+BSO3%+YOB at (a) 77K and (b) 65 K.

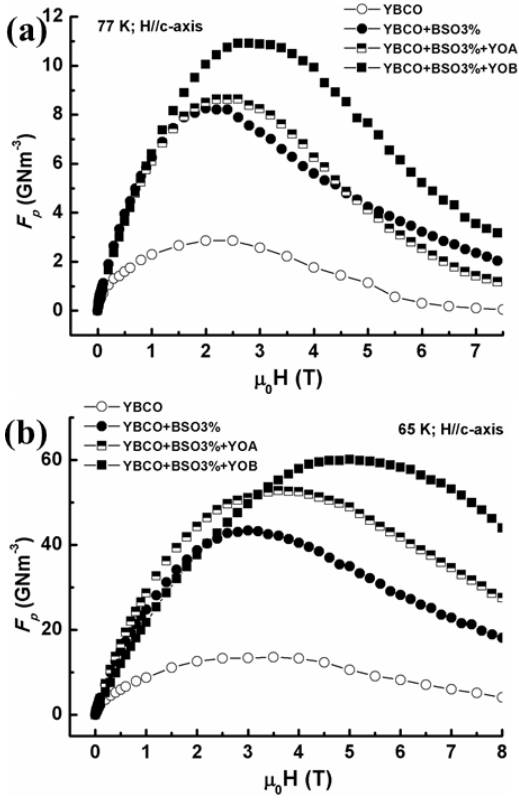


FIG. 3 Variation of  $F_p$  with applied magnetic field for YBCO, YBCO+BSO and YBCO+BSO+YO films at (a) 77K and (b) 65 K

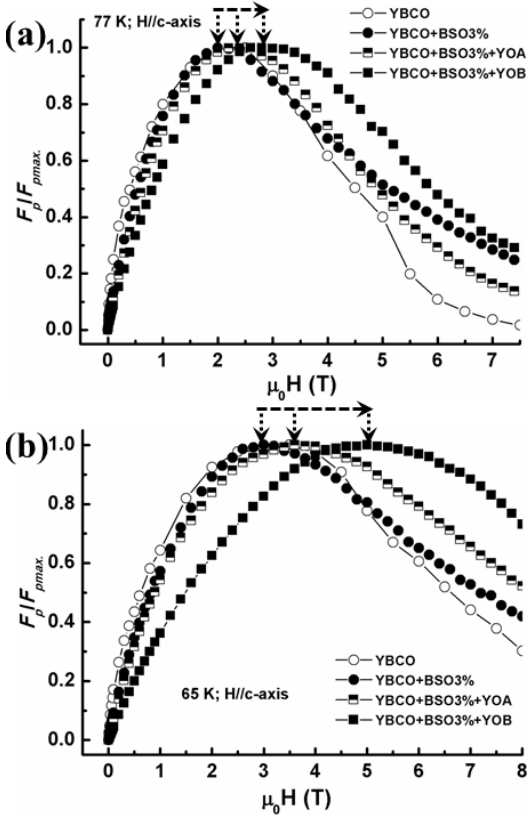
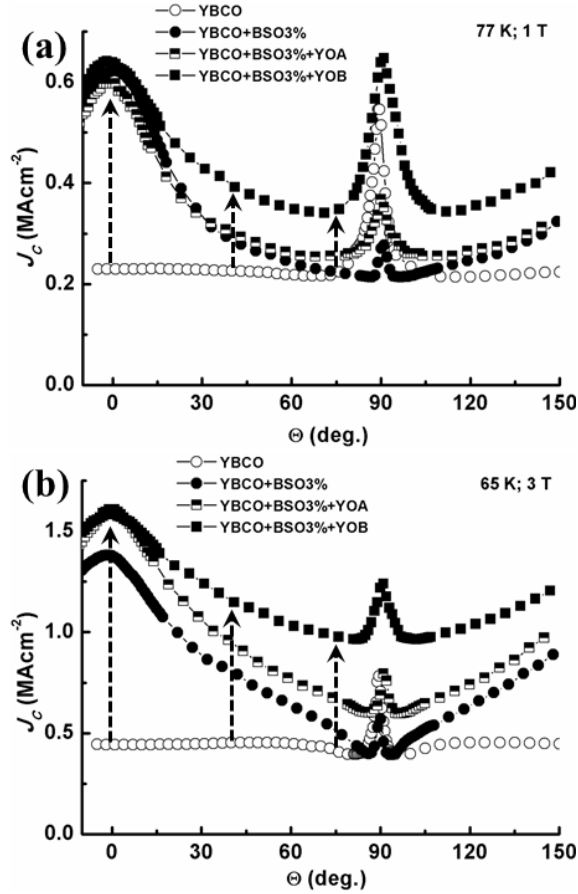


FIG. 4 Variation of reduced pinning force ( $F_p/F_{pmax}$ ) with applied magnetic field for YBCO, YBCO+BSO and YBCO+BSO+YO films at (a) 77K and (b) 65 K. Shifting of the  $F_{pmax}$  values is marked by dotted arrows.

(correlated disorder along the  $c$ -axis) till the applied magnetic field is less than or equal to the matching field. However, as the applied magnetic field keeps on increasing, the nanorods cannot accommodate any more vortices around them and here the nanoparticles start pinning the vortices as random pinning centers at places between the nanorods. Thus pinning force is provided by both the nanorods and the nanoparticles in the samples consisting of the hybrid APCs.

In the pristine YBCO film (without APC), pinning of the vortices take place due to naturally occurring defects such as point defects, oxygen vacancies, grain boundaries etc. These naturally occurring defects are weak in nature and cannot prevent the motion of the vortices at higher temperature and applied magnetic field. In the YBCO+BSO3% composite samples, however, pinning of vortices is caused mainly by BSO nanocolumns (strong pinning centers) apart from naturally occurring defects (weak pinning centers). It can be understood in rather simpler terms: the columnar defects hold the vortices much more strongly than weak pinning centers and the composite sample, therefore, can carry larger current against the Lorentz force than pristine YBCO sample at any applied magnetic field. Subsequently, the  $J_C$  at particular field and hence  $F_{pmax}$  value is enhanced. Even if the  $B_{max}$  value is the same,  $F_{pmax}$  of the composite sample is very high compared to that of pristine YBCO film. The comparison of  $B_{max}$  values for the composite samples (YBCO+BSO3%, YBCO+BSO3%+YOA and YBCO+BSO3%+YOB) is reasonable because in all cases pinning is dominantly caused by strong pinning centers and in these samples the density of strong pinning centers is varied systematically.  $B_{max}$  position shifts on the field axis as per the density of these strong pinning centers. Such a comparison between pristine YBCO and YBCO+BSO3% composite samples would not be reasonable because of the nature of dominant pinning centers: weak pinning center in the case of pristine YBCO and strong pinning centers in the case of YBCO+BSO3% composite samples.

Fig. 5 shows the angular dependence of  $J_C$  for YBCO, YBCO+BSO and YBCO+BSO+YO films measured at two different conditions: (a) 77 K, 1 T and (b) 65 K, 3 T. The improved angular dependent  $J_C$  behavior can be clearly observed in YBCO+BSO3% nanocomposite films where strong improvement in the  $c$ -axis correlated pinning has been resulted from continuous BSO nanocolumns. The samples consisting of hybrid APCs exhibit enhanced  $J_C$  values for all orientations of applied magnetic field due to cooperative contributions of both 1-D and 3-D APCs. Let us first consider the first case: 77 K, 1 T (fig. 5(a)). The incorporation of APCs resulted in 3-fold increase in the  $J_C$  value along the  $c$ -axis which is consequence of strong pinning of vortices by BSO nanocolumns. The significant increase in the  $J_C$  values is marked by upward arrows in the figure. It is noteworthy here that by adding and increasing the YO content, the  $c$ -axis peak remain unchanged. It may be understood in terms of BSO nanocolumns density in the samples containing APCs. Even though YO is added and its content is increased, the BSO concentration remains the same in all samples containing APCs. In the pristine YBCO film the strong  $J_C$  peak along the



**FIG. 5** Variation of  $J_c$  with the orientation of applied magnetic field with respect to the  $c$ -axis for YBCO, YBCO+BSO and YBCO+BSO+YO films at (a) 77 K, 1 T and (b) 65 K, 3 T.

ab-plane is observed because of its layered structure where the weak superconducting layers provide stability to the flux lines when these are parallel to the ab-plane [11]. In the YBCO+BSO3% sample, however, even if the  $c$ -axis  $J_c$  peak is enhanced significantly,  $J_c$  peak along  $ab$ -plane is suppressed somewhat presumably because of high density of continuous BSO nanorods which may prevent the intrinsic layer pinning [12]. As the content of YO is added and increased in the samples (hybrid APC samples), the  $J_c$  peak along the  $ab$ -plane also start becoming pronounced and stronger which means that pinning due to YO nanoparticles is compensating the loss of intrinsic pinning in the samples containing hybrid APC. Furthermore, in the intermediate angular regime,  $J_c$  improves ~2-fold in the YBCO+BSO+YOB sample which contains both BSO nanocolumns providing  $c$ -axis pinning and YO nanoparticles providing isotropic pinning. In the second case: 65 K, 3 T (fig.5(b)), the improvement in  $J_c$  is observed in all angular regimes in all samples except for the case of YBCO+BSO sample where  $J_c$  along the  $ab$  plane is found to be suppressed. As the YO nanoparticles added (YBCO+BSO+YOA), the enhancement is observed for all angular regime and further increasing the YO content (YBCO+BSO+YOB), the enhancement is most prominent especially in the intermediate angular regime indicating the

role of YO nanoparticles providing strong isotropic pinning. Although there is enhancement in the  $J_c$  values in the intermediate angular regime for YBCO+BSO+YOA sample, the enhancement is more prominent in YBCO+BSO+YOB sample. It is to be noted here that the YO nanoparticles have been incorporated into the YBCO matrix by means of surface modified targets and the area of the YO sector pieces are estimated to be 2.2%(A) and 3%(B). The volume concentration of the YO nanoparticles in the hybrid APC samples may be different from these numbers (laser spot being elliptical and YO pieces being circular sector in shape). Also the inhomogeneous distribution of YO nanoparticles in these samples cannot be ignored.

The reduction of  $J_c$  by changing the applied magnetic field orientation has been described by Paulius *et al.* [13]. According to their model, when the magnetic field is oriented at an angle with the  $c$ -axis of the samples, a vortex line which is trapped in the columnar defect has three different regions: a trapped portion of the vortex occupied by the columnar defect and two healing regions relatively free from the columnar defect. As the inclination of the magnetic field with respect to  $c$ -axis increases, the length of the trapped portion of the vortex decreases and subsequently  $J_c$  becomes low. At sufficient inclination, no region of the vortex is trapped and  $J_c$  becomes minimum. In the present case of samples consisting of hybrid APCs, even though the vortices can become free of the BSO columnar disorders in the intermediate angular regime, the YO nanoparticles can pin different portions of the vortices irrespective of the orientation of the applied magnetic field which results in the improved  $J_c$  values along all the magnetic field orientations. It, therefore, can be concluded that the combination of 1D+3D APCs is very useful in improving the vortex pinning properties of YBCO films which can be observed in terms of increased  $F_{pmax.}$  values, shifting of  $F_{pmax.}$  towards higher applied magnetic fields and improvement of  $J_c$  values along all the orientations of the applied magnetic field.

#### IV. CONCLUSIONS

We have successfully incorporated hybrid APCs into YBCO film matrix and demonstrated that the hybrid APCs improve the vortex pinning properties of YBCO film significantly. At both the temperatures: 77 K and 65 K, the  $F_{pmax.}$  values exhibited systematic increase with increasing the density of hybrid APCs and it also shifted towards higher magnetic field indicating more effective vortex pinning at higher applied magnetic field. The shifting of the  $F_{pmax.}$  values towards higher applied magnetic field has been attributed to the strong pinning of vortices by YO nanoparticles. The angular dependence of  $J_c$  exhibited significant improvement in the YBCO film with hybrid APCs not only along the  $c$ -axis but also along the entire investigated angular regime. The BSO nanocolumns (1-D APCs) are supposed to pin the vortices when the flux lines are along the  $c$ -axis whereas, YO nanoparticles (3-D APCs) supposedly pinned the vortices isotropically, resulting in enhanced  $J_c$  values along all the orientations of the applied magnetic fields.

## REFERENCES

- [1] K. Matsumoto, and P. Mele, "Artificial pinning center technology to enhance vortex pinning in YBCO coated conductors," *Supercond. Sci. Technol.*, vol. 23, 014001, 2010.
- [2] P. Mele, K. Matsumoto, T. Horide, A. Ichinose, M. Mukaida, Y. Yoshida, and S. Horii, "Insertion of nanoparticulate artificial pinning centers in  $\text{YBa}_2\text{Cu}_3\text{O}_{7-x}$  films by laser ablation of a  $\text{Y}_2\text{O}_3$  surface modified target," *Supercond. Sci. Technol.*, vol. 20, pp. 616-620, 2007.
- [3] T. Haugan, P. N. Barnes, R. Wheeler, F. Meisenkothen, and M. Sumption, "Addition of nanoparticle dispersions to enhance flux pinning of the  $\text{YBa}_2\text{Cu}_3\text{O}_{7-x}$  superconductor," *Nature*, vol. 430, pp. 867-870, 2004.
- [4] J. L. M. Driscoll, S. R. Foltyn, Q. X. Jia, H. Wang, A. Serquis, L. Civale, B. Maiorov, M. E. Hawley, M. P. Maley, and D. E. Peterson, "Strongly enhanced current densities in superconducting coated conductors of  $\text{YBa}_2\text{Cu}_3\text{O}_{7-x} + \text{BaZrO}_3$ ," *Nat. Mater.*, vol. 3, pp. 439-443, 2004.
- [5] A. Goyal, S. Kang, K. J. Leonard, P. M. Martin, A. A. Gapud, M. Varela, M. Paranthaman, A. O. Ijaluola, E. D. Specht, J. R. Thompson, D. K. Christen, S. J. Pennycook, and F. A. List, "Irradiation-free, columnar defects comprised of self-assembled nanodots and nanorods resulting in strongly enhanced flux-pinning in  $\text{YBa}_2\text{Cu}_3\text{O}_{7-\delta}$  films," *Supercond. Sci. Technol.*, vol. 18, pp. 1533-1538, 2005.
- [6] C. V. Varanasi, J. Burke, H. Wang, J. H. Lee, and P. N. Barnes, "Thick  $\text{YBa}_2\text{Cu}_3\text{O}_{7-x} + \text{BaSnO}_3$  films with enhanced critical current density at high magnetic fields," *Appl. Phys. Lett.*, vol. 93, 092501, 2008.
- [7] P. Mele, K. Matsumoto, A. Ichinose, M. Mukaida, Y. Yoshida, S. Horii, and R. Kita, "Systematic study of  $\text{BaSnO}_3$  insertion effect on the properties of  $\text{YBa}_2\text{Cu}_3\text{O}_{7-x}$  films prepared by pulsed laser ablation," *Supercond. Sci. Technol.*, vol. 21, 125017, 2008.
- [8] D. M. Feldmann, T. G. Holesinger, B. Maiorov, S. R. Foltyn, J. Y. Coulter, and I. Apodaca, "Improved flux pinning in  $\text{YBa}_2\text{Cu}_3\text{O}_7$  with nanorods of the double perovskite  $\text{Ba}_2\text{YNbO}_6$ ," *Supercond. Sci. Technol.*, vol. 23, 095004, 2010.
- [9] A. K. Jha, K. Matsumoto, T. Horide, S. Saini, P. Mele, Y. Yoshida and S. Awaji, "Tuning the microstructure and vortex pinning properties of YBCO based superconducting nanocomposite films by controlling the target rotation speed" *Supercond. Sci. Technol.*, vol. 27, 025009, 2014.
- [10] T. Horide, T. Kawamura, K. Matsumoto, A. Ichinose, M. Yoshizumi, T. Izumi, and Y. Shiohara, " $J_c$  improvement by double artificial pinning centers of  $\text{BaSnO}_3$  nanorods and  $\text{Y}_2\text{O}_3$  nanoparticles in  $\text{YBa}_2\text{Cu}_3\text{O}_7$  coated conductors," *Supercond. Sci. Technol.*, vol. 26, 075019, 2013.
- [11] M. Tachiki, and S. Takahashi, "Anisotropy of critical current in layered oxide superconductors," *Sol. St. Comm.*, vol. 72, pp. 1083-1086, 1989.
- [12] G. Ercolano, S. A. Harrington, H. Wang, C. F. Tsai, and J. L. M. Driscoll, "Enhanced flux pinning in  $\text{YBa}_2\text{Cu}_3\text{O}_{7-\delta}$  thin films using Nb based double perovskite additions," *Supercond. Sci. Technol.*, vol. 23, 022003, 2010.
- [13] L. M. Paulius, J. A. Fendrich, W.-K. Kwok, A. E. Koshelev, V. M. Vinokur, G. W. Crabtree, and B. G. Glagola, "Effects of 1-GeV uranium ion irradiation on vortex pinning in single crystals of the high-temperature superconductor  $\text{YBa}_2\text{Cu}_3\text{O}_{7-\delta}$ ," *Phys. Rev. B*, vol. 56, pp. 913-924, 1997.